land

MDPI

Article

Construction of Ecological Security Patterns and Evaluation of Ecological Network Stability under Multi-Scenario Simulation: A Case Study in Desert–Oasis Area of the Yellow River Basin, China

Wenhao Cheng [1,2], Caihong Ma [2,*], Tongsheng Li [1] and Yuanyuan Liu [2]

[1] College of Urban and Environment Sciences, Northwest University, Xi'an 710127, China; chengwh@nxu.edu.cn (W.C.); leetang@nwu.edu.cn (T.L.)
[2] College of Geography and Planning, Ningxia University, No.539 Helanshan West Road, Yinchuan 750021, China; 12022130985@stu.nxu.edu.cn
* Correspondence: mchyanni@nxu.edu.cn

Abstract: Land use change has a significant impact on the sustainability of ecosystems, and ecological security patterns (ESPs) can improve environmental quality through spatial planning. This study explored a multi-scenario ESP framework by integrating future land use simulation (FLUS) and minimum cumulative resistance (MCR) for urban agglomeration along the Yellow River Basin (YRB) in Ningxia. The research involved simulating land use change in 2035 under four development scenarios, identifying ecological security networks, and evaluating network stability for each scenario. The study revealed that the ecological sources under different development scenarios, including a natural development scenario (NDS), an economic development scenario (EDS), a food security scenario (FSS), and an ecological protection scenario (EPS), were 834.82 km^2, 715.46 km^2, 785.56 km^2, and 1091.43 km^2, respectively. The overall connectivity values (O_G) for these scenarios were 0.351, 0.466, 0.334, and 0.520, respectively. It was found that under an EPS, the ESPs had the largest area of ecological sources and the most stable ecological network structure, which can effectively protect natural habitats. This study provides a valuable method for identifying ESPs that can respond to diversity and the uncertainty of future development. It can assist decision-makers in enhancing the ecological quality of the study area while considering various development scenarios.

Keywords: ecological protection; scenario analysis; minimum cumulative resistance; ecological stability evaluation; Yellow River Basin

check for updates

Citation: Cheng, W.; Ma, C.; Li, T.; Liu, Y. Construction of Ecological Security Patterns and Evaluation of Ecological Network Stability under Multi-Scenario Simulation: A Case Study in Desert–Oasis Area of the Yellow River Basin, China. *Land* **2024**, *13*, 1037. https://doi.org/10.3390/land13071037

Academic Editor: Brian D. Fath

Received: 22 May 2024
Revised: 5 July 2024
Accepted: 9 July 2024
Published: 10 July 2024

Copyright: © 2024 by the authors. Licensee MDPI, Basel, Switzerland. This article is an open access article distributed under the terms and conditions of the Creative Commons Attribution (CC BY) license (https://creativecommons.org/licenses/by/4.0/).

1. Introduction

With rapid increases in economic development and urbanization, land use has undergone unprecedented change, leading to a significant disruption of the ecosystem [1]. This has resulted in landscape fragmentation, urban heat islands, and biodiversity loss, all of which directly or indirectly affect the stability and sustainability of ecological patterns [2,3]. Therefore, the construction of ecological security pattern (ESP) and the evaluation of ecological quality have been developed to address regional ecological issues and provide valuable support for regional management and planning [4].

The establishment of ESP, derived from landscape ecological planning and combined with land use patterns for the construction and optimization of ecological networks, serves as an efficient spatial pathway for balancing ecological conservation and socioeconomic development [5]. Currently, ESP research has evolved into a general paradigm of "identifying the source areas, constructing the resistance surfaces, and extracting the corridors" [6]. There are two major approaches to identify ecological sources: structure-oriented methods,

which considers the structural connectivity between different patches [7], and function-oriented methods, which are based on the significance of the indicators; patches with high ecological significance are identified as different from the surrounding landscape matrix [8]. Compared to function-oriented methods, structure-oriented methods used for establishing ESPs have been demonstrated to enhance network connectivity despite changes in scale [9]. The MSPA approach is widely utilized, as it automatically classifies the pixel data of focal feature classes into a new structural connectivity feature class [10]. When assessing ecological resistance surfaces, a comprehensive resistance surface map is created using the analytic hierarchy process (AHP) and Delphi method, which have supplemented expert-assigned resistance values [11]. Ecological corridors are key channels for ecological flow and diffusion, and the minimum cumulative resistance (MCR) model has been extensively applied because it considers landscape heterogeneity and horizontal connections between landscape units [12]. However, the construction of ESP based on the current perspective often fails to reflect spatiotemporal variations in the impacts of natural and artificial factors on the landscape. Models such as the future land use simulation (FLUS) can utilize self-adaptive inertia and competition mechanisms to analyze the complexities and indeterminacies of interactions and competition among different land types, offering better support for simulating future land use change across various periods and scenarios [13]. Gradually, an increasing number of studies have simulated future ESPs by exploring potential ecological sources and corridors. It subsequently offers recommendations for the restoration and optimization of ecological networks.

The evaluation of ESP quality is a prerequisite for enhancing the structural stability of the landscape. Based on graph theory, the metrics used to evaluate ESPs for structure-oriented methods can be classified into centrality metrics and connectivity metrics. Centrality metrics describe the centrality degree and comprehensive influence of a local area in the overall network, such as the K_p index, L_p index, and M_p index [14]. Connectivity metrics reflect the ecological process and ecological connection degree of the landscape, such as the α index, β index, γ index, and G index [15]. Shen and Wu developed the evaluation system to refer to the aspects of centrality and connectivity. It contained the indexes of average node degree (k), average shortest path (I), global efficiency (E_G), and clustering coefficient (cc). Moreover, an overall value (O_G) was introduced to comprehensively quantify the structure of the ESPs, representing an equally weighted result of the assessment of k, I, E_G, and cc [9].

The Yellow River Basin (YRB) is the cradle of Chinese civilization and has played a crucial role in maintaining ecological and socioeconomic sustainability [16]. The urban agglomeration along the YRB in Ningxia is a unique desert–oasis area, and holds strategic importance for ensuring stability in the northwestern Chinese frontier. However, due to fragile natural conditions and extensive development, human–land conflict relationships have emerged as a major challenge [17,18]. Therefore, it is necessary to undertake the construction and optimization of the ESPs of urban agglomeration along the YRB in Ningxia as a urgent task in the future [19]. Given the complexity and uncertainty of future development, the land use change and ESP construction could potentially impact a range of various future scenarios. Hence, we attempted to solve this knowledge gap by addressing two key scientific inquiries: how can we predict future land use change under various scenarios, and how can we construct and evaluate ESPs? With a focus on these questions, this study developed a multi-scenario ESP framework to accommodate future land use through the integration of FLUS and MCR models. The major objectives of this study were as follows: (1) to simulate land use change under various scenarios in 2035, the year when China is projected to reach peak urbanization, using the FLUS model; (2) to develop the ESPs by identifying ecological sources through MSPA and landscape connectivity analysis (LCA), as well as extracting ecological corridors using MCR and gravity models; and (3) to assess the stability of the ESPs from comprehensive perspectives.

2. Materials and Methods

2.1. Study Area and Data

2.1.1. Study Area

The Ningxia Hui Autonomous Region is located in the upper reach of the YRB in northwestern China, ranging from 104°17′–107°39′ E longitude and 35°14′–39°23′ N latitude. It is characterized as a temperate continental climate and classified as an arid or semiarid region. Based on the guiding document, *Development Plan of the Urban Belt along the Yellow River Economic Zone*, the urban agglomeration along the YRB in Ningxia includes 13 counties (districts) (Figure 1), with a total area of 22,700 km^2, a resident population of 5.05 million and a GDP of 44.95 billion US dollars in 2020. Although the study area only represents 34.2% of the total area in Ningxia, it accounts for 70.1% of the population and 88.2% of the GDP. The region is traversed by the Yellow River from southwest to northeast, creating several wetland parks with diverse biodiversity [20,21], despite being bordered by the Tengger Desert, Ulan Buh Desert, and Mu Us Sandy Land. It is delineated by Qingtong Canyon into the Yinchuan Plain in the north and the Weining Plain in the south. The primary land use types are grassland and cropland, which make up 45.8% and 24.4%, respectively. Other land use types, such as unused land, construction land, forestland, and water body, account for 10.6%, 8.4%, 5.6%, and 5.1%, respectively. The forestland and water body are classified as the ecological land use types, providing the foods and habitats for different kinds of mammals, birds, and fishes. It promotes biological diversity by species diffusion. Cropland is primarily utilized to produce grain and meat for human beings. Construction land, including urban and rural transportation land types, serves as the main location for human activities. Grassland is used for grazing or remains unused due to low vegetation cover in arid and semi-arid regions.

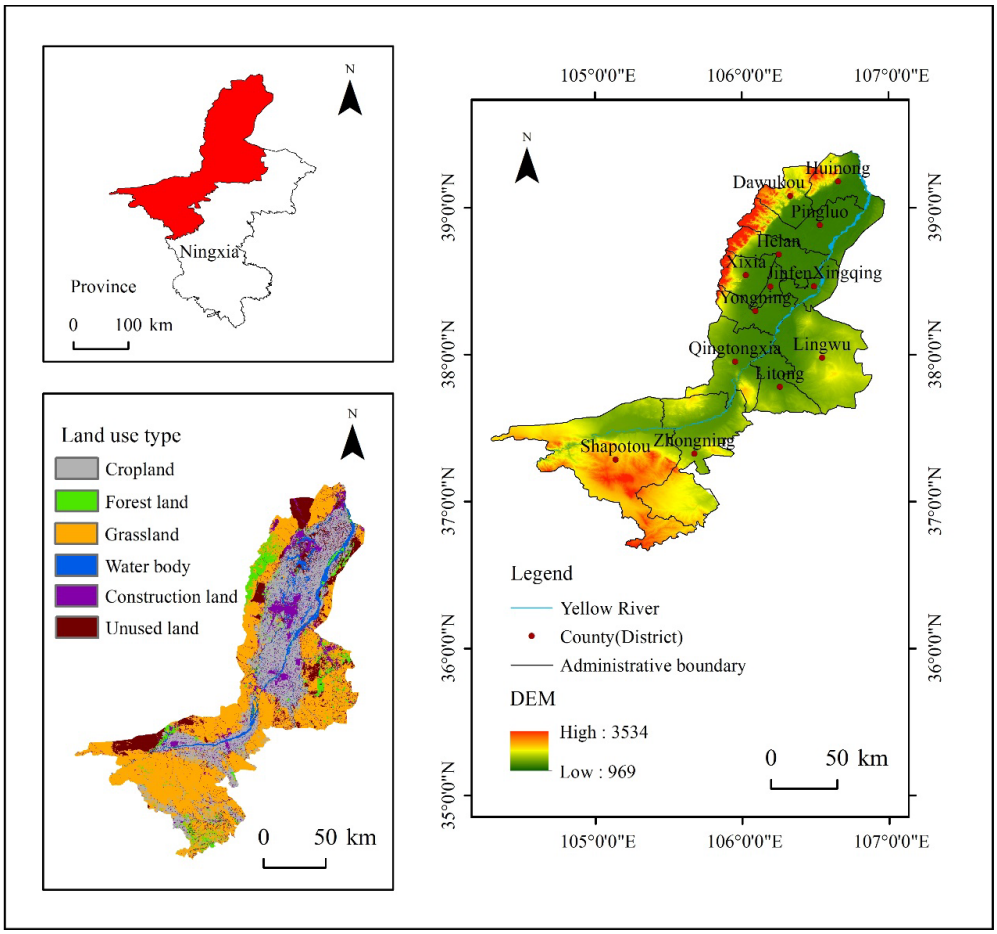


Figure 1. Study area.

2.1.2. Data Sources and Processing

The main data and their formats, sources and other key information were shown in Table 1. In this study, the land use types were divided into six categories: cropland, forestland, grassland, water body, construction land and unused land. The grids used here were resampled to 90 m × 90 m for further calculation.

Table 1. Main data used in the study.

Data	Format	Source
Land use type	Vector data in 2020	Department of Ningxia Nature Resource
Digital elevation model (DEM)	Grid at 30 m in 2020	http://www.gscloud.cn/
Slope	Grid at 90 m in 2020	http://www.gscloud.cn/
Soil erosion	Grid at 1000 m in 2020	http://www.resdc.cn
NDVI	Grid at 1000 m in 2020	http://www.resdc.cn
Road and railway	Line in 2020	http://openstreetmap.org/
River	Line in 2020	http://openstreetmap.org/
Population density	Grid at 1000 m in 2019	http://www.worldpop.org/
GDP density	Grid at 1000 m in 2019	http://www.resdc.cn
Night light data	Grid at 1000 m in 2019	http://www.resdc.cn
Precipitation	Point in 2011–2020	http://www.cma.cn/
Administrative boundary	Polygons in 2020	http://www.hydrosheds.org/

2.2. Methods

The flowchart of this study is shown in Figure 2, which consists of three major steps: multi-scenario land use simulation (see Section 2.2.1), ESP construction (see Section 2.2.2), and ESP network connectivity evaluation (see Section 2.2.3).

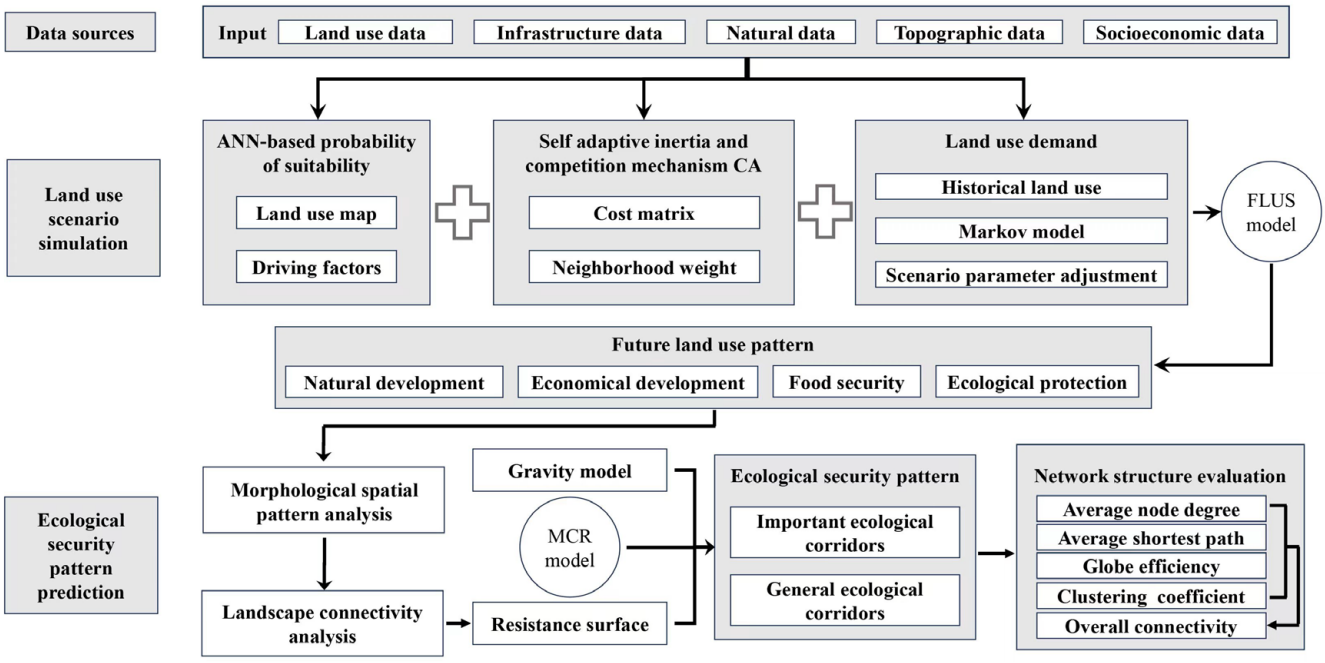


Figure 2. Framework of the integration of future ecological security patterns (ESPs) for land use simulation.

2.2.1. Land Use Simulation under Multiple Scenarios

The FLUS model, based on the traditional cellular automata principle (CA-Markov), can effectively simulate future land use change. It contains three modules: (1) an artificial neural network (ANN) algorithm to obtain the transition probability of each type; (2) self-adaptive internal and competition mechanisms to analyze the mutual competition and

interaction between land use types according to a transfer matrix; and (3) a Markov model to predict the demand of future land use types [13,22].

Transition Probability of Land Use Change

The transition probability of land use change is calculated in the output layer using the ANN algorithm combined with driving factors. The equations are as follows [22,23]:

$$p(p,k,t) = \sum_j w_j k \times sigmoid\left(net_j(p,t)\right)$$

$$sigmoid\left(net_j(p,t)\right) = \frac{1}{1+e^{-net_j(p,t)}} \qquad net_j(p,t) = \sum_i w_{ij} \times \left(x_j(p,t)\right)$$

where $p(p,k,t)$ means the transition probability of land use type k on grid p at time t; w_j k means the weight between layers of hidden and output; sigmoid means the function; $net_j(p,t)$ means the receipt signal of neuron j; w_{ij} means the weight between layers of hidden and input; and $x_i(_{p,t})$ is the variable of input neuron i.

The total probability from one type converted to another is computed as follows [24]:

$$TP^t_{p,k} = P^t_{p,k} \times \alpha^t_{p,k} \times Inertia^t_k \times (1 - SC_{c \to k})$$

where $TP^t{}_{p,k}$ means the total probability from one land use type to another land use type k on grid p at time t; $a^t{}_{p,k}$ means neighborhood effect; $Inertia^t{}_k$ means the inertia coefficient from one land use type to type k; $SC_{c \to k}$ means the cost from c to k.

Considering the existing research results and the specific situation in the study area [19,22], seven factors, namely the DEM, slope, NDVI, nightlight index, distance from roads, GDP and population density, were selected to calculate the probability of land suitability.

FLUS Models' Parameter Setting

The parameter setting for the self-adaptive internal and competition mechanisms of CA contains the land use transfer matrix, and neighborhood effect.

The land use transfer matrix is used to express the mutual conversion of land use types [25]. A value of 1 indicates that a land type could be converted, and a value of 0 indicates the opposite. The land use transfer matrices were determined according to the actual conditions of the urban agglomeration along the YRB in Ningxia (Table 2).

Table 2. Land use transfer matrices of the four scenarios.

	NDS					**EDS**					**FSS**					**EPS**				
	a	**b**	**c**	**d**	**e**	**a**	**b**	**c**	**d**	**e**	**a**	**b**	**c**	**d**	**e**	**a**	**b**	**c**	**d**	**e**
a	1	1	0	1	1	1	1	0	1	1	1	0	0	0	0	1	1	0	1	1
b	1	1	0	1	1	1	1	0	1	1	1	1	0	1	1	0	1	0	1	0
c	1	1	1	1	1	1	1	1	1	1	1	1	1	1	1	0	1	1	1	0
d	1	1	0	1	1	1	1	0	1	1	1	1	0	1	1	0	1	0	1	0
e	1	1	0	1	1	0	0	0	0	1	1	0	0	0	1	0	1	0	1	1

Note: a–e represent cropland, forestland, grassland, water body and construction land, respectively. Under the four scenarios, the transfer directions between unused land and other land use types were the same: unused land could be converted to other land use types, but other land use types could not be converted to unused land.

The neighborhood effect not only directly reflects the expansion intensity of land use types but also reflects the expansion ability of each land use type driven by external factors [26]. Within the range of 0–1, the higher the value is, the greater the capacity for expansion. The neighborhood weights of each land use type were designed based on related literature and expert knowledge (Table 3).

Table 3. Neighborhood effect of each land use type.

Type	Cropland	Forestland	Grassland	Water Body	Construction Land	Unused Land
Coefficient	0.5	0.5	0.2	0.3	0.8	0.1

Forecasting Land Use Demand under Multiple Scenarios

The Markov model can be utilized for trend prediction by analyzing the initial probability of various land use changes and the transition probability between different land use changes. The quantity of land use in the future is computed as follows [27]:

$$S_{(t+1)} = P_{ij} \times S_{(t)}$$

where the $S_{(t)}$ and $S_{(t+1)}$ are the land use transfer matrices at time t and $t + 1$; P_{ij} is the transition from type i to j.

Referring to relevant studies, we established four development scenarios in this study [22], which integrated the current natural and social conditions of the study area with the spatial planning and environmental conservation policy of the YRB: (1) the natural development scenario (NDS), based on the tendency of historical land use and predicting future land use; (2) the economic development scenario (EDS), which prioritized economic development and accelerated urban–rural integration, resulting in a 40% increase in conversion to construction land and a 10% reduction in other land types; (3) the food security scenario (FSS), which strictly protected cropland, resulting in a 30% increase in the likelihood of conversion to this land use type and a 10% reduction in conversion to other land use types; and (4) the ecological protection scenario (EPS), which prioritized ecological security, cropland, and construction land in accordance with the NDS, leading to a 40% increase in the likelihood of conversion to forestland and water body and a 10% reduction in conversion to other land use types. Forestland was considered as the restricted area in the first three scenarios, while forestland, water body, and natural reserves were designated as the restricted areas in the EPS.

Model Validation

The kappa coefficient is an important indicator to test the accuracy of land use prediction and is used to assess the consistency between simulated and actual land use data. A kappa value exceeding 0.8 indicates a high level of consistency [28]. The simulation consistency was validated against real land use data for 2015–2020, resulting in a kappa coefficient of 86.52% (an overall accuracy of 90.47%).

2.2.2. ESP Construction

Ecological Source Identification

The morphological spatial pattern analysis (MSPA) method is a mapping algorithm based on the principle of mathematical morphology that uses erosion, expansion, open operation, and closed operation to determine the spatial pattern of raster images [29]. For this study, two values were generated, with forestland and water body used as foreground data and other land use types utilized as background data. The binary raster data were imported into Guidos Toolbox 3.0 software using the eight-neighborhood analysis method [30]. The edge width was set to the default value of "1", the transition was set to the default value of "off", and intext was set to the default value of "on". Finally, the land use types were classified into 7 basic spatial elements: core, islet, perforation, edge, loop, bridge, and branch. The core consists of large, more complete habitat patches, that were selected as alternative ecological patches.

Landscape connectivity analysis (LCA) illustrates the continuity of a landscape's spatial structure and can calculate how easy or difficult it is for organisms to move between ecological patches in a special field [31,32]. Based on the MSPA results, Conefor 2.6 software was used to further select habitat patches with good ecological functions, good development

trends, internal homogeneity, and the ability to spread in all directions. Finally, the core areas larger than 2 km^2 were selected to quantitatively measure the patch connectivity index (*dIIC*) and patch importance index (*dPC*), allowing for the ranking of the patches in terms of importance. The higher the *dPC* index is, the greater the importance of the patch, and numerous core patches that can be used as ecological sources were extracted accordingly. The equations are as follows [7,19]:

$$dIIC = \frac{\sum_{i=1}^{n}\sum_{j=1}^{n}\frac{a_i a_j}{1+nl_{ij}}}{A_L^2} \qquad dPC = \frac{PC - PC_{remove}}{PC} * 100\%$$

where *dIIC* denotes the connectivity probability, n denotes the number of total patches, a_i and a_j denote the respective areas of patches i and j, l_{ij} denotes the maximum diffusion probability between patch i and patch j, and A_L denotes the total area of the study region. PC_{remove} is the connectivity probability of the remaining patches after removing a patch, and *dPC* indicates the degree of importance of the patch. Finally, the patches in the *dPC* index which they were greater than 0.2 were selected as the ecological sources.

Resistance Surface Establishment

The key to accurately characterizing ESPs is taking reasonable approach to estimating its ecological resistance value. This value should not only reflect the horizontal resistance of ecological processes but also represent the challenges faced by a species when moving through the landscape [33]. Based on the selection of previous resistance factors [19,34], and according to the condition of study area and the data that can be obtained easily, we selected seven resistance indicators, including land use, DEM, slope, soil erosion, NDVI, distance from roads, and distance from rivers. The ecological resistance factors were reclassified into five levels, assigned as 10, 30, 50, 70, and 90, and the weights of the seven factors were determined using AHP (Table 4). Finally, the resistant surfaces were reclassified into five levels: lower, low, medium, high and higher; the lower the resistance level was, the weaker the impact of external disturbance on the ecosystem [35].

Table 4. Resistance values and weights of the ecological resistance factors.

Evaluation	Resistance Value					Weight
	10	30	50	70	90	
Land use	Forestland	Grassland, Cropland	Water body	Unused land	Construction land	0.302
DEM (m)	<1234	1235–1478	1479–1767	1768–2204	>2205	0.120
Slope (°)	<2.89	2.90–7.76	7.77–15.47	15.48–26.17	26.17–61.78	0.165
Soil erosion	Normal	Mild	Moderate	High	Extremely	0.176
NDVI	0.70–0.99	0.51–0.69	0.35–0.50	0.29–0.34	0.00–0.28	0.145
Distance from roads (m)	>2051	1051–2050	551–1050	51–550	100 (itself)	0.046
Distance from rivers (m)	>7001	5001–7000	3001–5000	1001–3000	2000 (itself)	0.042

Ecological Corridor Extraction

The MCR model is widely applied to extract ecological corridors, as it can compute the cost of species migration from a source to a target. The equation is as follows [36]:

$$MCR = fmin\sum_{i=1}^{m}\sum_{j=1}^{n} D_{ij}R_i$$

where *MCR* denotes the minimum cumulative resistance; f indicates the positive correlation function between the minimum cumulative resistance and the ecological process; D_{ij}

indicates the spatial distance traversed by source i to unit j; and R_i indicates the resistance coefficient of the unit to species diffusion. The corridors were obtained by the GIS distance model for our study.

The gravity model is utilized to categorize ecological corridors, with the significance of these corridors being measured by the ecological gravitational force between different patches. The greater the value of the ecological gravitational force between two patches, the higher the importance of the ecological corridors. The equation is as follows [37]:

$$G_{ab} = \frac{N_a N_b}{D_{ab}^2} = \left(\frac{1}{p_a} \times lnS_a\right)\left(\frac{1}{p_b} \times lnS_b\right) / \left(\frac{L_{ab}}{L_{max}}\right)^2$$

where G_{ab} is the mutual force between patches a and b; D_{ab} is the normalized value of the resistance of the ecological corridors between two ecological sources; and $N_a(N_b)$, $p_a(p_b)$, and $S_a(S_b)$ are the weight, resistance value and area of ecological source $a(b)$, respectively. L_{ab} is the cumulative resistance value of ecological sources a and b, and L_{max} is the maximum resistance value. In this study, corridors with mutual forces > 10,000 between patches were considered important corridors, and those with mutual forces ranging from 5000–10,000 between patches were considered general corridors.

2.2.3. ESPs Stability Evaluation

The Ucinet and Pajek tools are applied to abstract ESPs into complex networks, and to explore the structural characteristics of the establishment of various ESPs in terms of metric change. The metrics are composed of nodes and lines representing landscape entities (ecological sources and corridors). The metrics system was summarized in Table 5 via the integration of previous works by Shen and Wu [9].

Table 5. Metrics for quantifying the stability of ESPs.

Metric	Equation	Description	Type	References
Average node degree (k)	$k = \frac{1}{N}\sum_{i \neq j \in G} a_{ij}$	K describes the average node degree of nodes in network G, N is the number of total nodes, a_{ij} is the number of nodes i directly connected to nodes j; a higher k value indicates a better the convenience between nodes.	Centrality	[38,39]
Average shortest path (I)	$I = \frac{2}{N(N-1)}\sum_{i \neq j \in G} d_{ij}$	I denotes the migration cost among different nodes, which is negatively correlated with connectivity, and d_{ij} is the distance of the shortest path connecting the nodes.	Connectivity	[40]
Global efficiency (E_G)	$E_G = \frac{1}{N(N-1)}\sum_{i \neq j \in G} \frac{1}{d_{ij}}$	E_G refers to the efficiency of movement in the whole network, which can avoid the divergence of the I index; the higher the E_G index is, the less energy is consumed for moving between nodes.	Centrality	[41,42]

Table 5. *Cont.*

Metric	Equation	Description	Type	References
Clustering coefficient (*cc*)	$cc = \frac{1}{N}\sum_{i=1}^{N}\frac{2E_i}{k_i(k_{i-1})}$	*cc* measures the agglomeration degree of nodes in network *G*, E_i is the actual number of connecting lines between the neighboring nodes of node *i*, and k_i is the degree of node *i*; a higher *cc* value indicates a higher agglomeration of network *G*.	Connectivity	[34,43]
Overall connectivity (O_G)	$O_G = \left(k^{/} + \frac{1}{I^{/}} + {E_G}^{/} + cc^{/}\right)/4$	The O_G denotes the overall connectivity of network *G*, which is the equally weighted result of the assessment of *k*, *I*, E_G and *cc*; $k^{/}$, $I^{/}$, ${E_G}^{/}$, $cc^{/}$ are the normalized values of the four metrics; the higher O_G value is, the better the comprehensive stability.	Comprehensiveness	[9]

3. Results

3.1. Land Use Simulation under Multiple Scenarios

Figure 3 depicts the transition probability matrix of land in the study area from 2015–2020. The primary change in land use involved a conversion of 11.39% of cropland and 24.01% of grassland into construction land due to rapid urbanization. It also showed that 37.34% of cropland and 40.84% of construction land were converted into forestland or water body for ecological protection and human welfare, and 40.46% of unused land was converted into cropland to meet the requirement for a minimum cropland area exceeding 120,000,000 hectares in China.

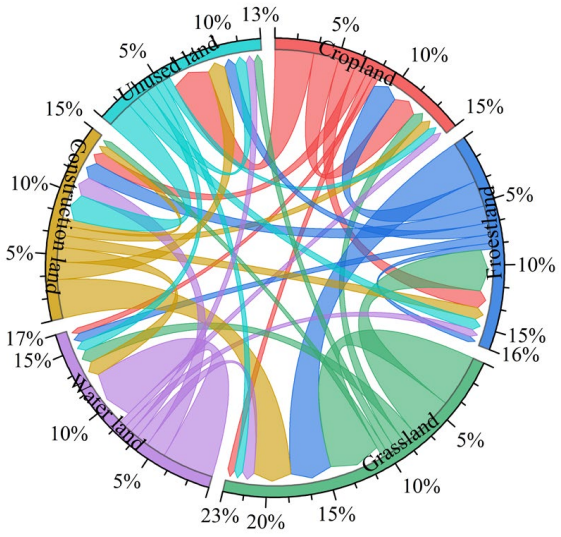


Figure 3. Land use transfer probability matrix for 2015–2020.

Table 6 and Figure 4 display the quantities and spatial distributions of land use types under the multiple scenarios simulation in 2035. Grassland and cropland remained the predominant land use types, subjected to the average annual precipitation of nearly 200 mm and strong evaporation. Meanwhile, the presence of the Yellow River throughout the region ensured sufficient water resources for agricultural production. The spatial distributions of forestland and water body were similar across the four scenarios. Forestland was concentrated in the nature reserves and forest farms. These regions were located at

the altitudes 1200–1800 m, which have suitable factors for macrophanerophytes, such as sunlight, temperature, precipitation, and soil fertility. Water body was distributed in the mainstream and its tributaries of the Yellow River, as well as in lakes and wetlands in Yinchuan Plain. The terrain of Weining Plain resulted in a narrower main stream of the Yellow River compared to that in Yinchuan Plain, which in turn caused fewer oxbow lakes. The differences among the various scenarios were the areas and scales of the patches. These differences can be attributed to the distinct development aims and strategies, resulting in varying proportions of each land use type across the scenarios. For instance, urban expansion in the EDS led to larger areas of construction land at the expense of cropland, while the FSS prioritized cropland protection. Furthermore, there was a decrease in ecological security land use types under NDS, EDS, and FSS scenarios but an increase under EPS from 2020 to 2035.

Table 6. Area (km^2) of various land use types under multiple years/scenarios.

Year/Land Use Type	2015	2020	NDS in 2035	EDS in 2035	FSS in 2035	EPS in 2035
Cropland	5372	5532	5861	5276	7620	5861
Forestland	1298	1270	1211	1090	1090	1696
Grassland	10,512	10,378	10,000	9000	9000	9000
Water body	1203	1157	1147	1037	1037	1605
Construction land	1758	1901	2220	3108	1994	2220
Unused land	2496	2403	2198	1979	1978	1978

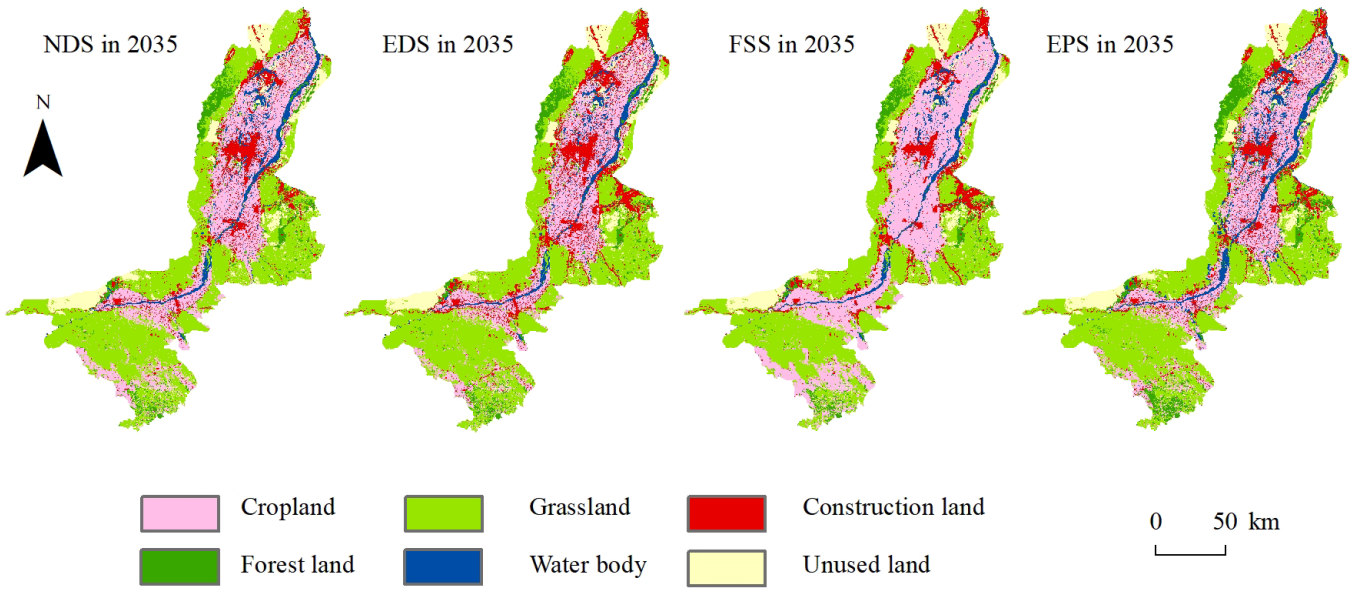


Figure 4. Distribution of land use types under the simulation of multiple scenarios.

3.2. ESP Identification

3.2.1. Ecological Sources

The spatial patterns of the ecological patches under multiple scenarios were displayed in Figure 5. The numbers of ecological sources in the study area were 20, 12, 17, and 15 under the NDS, EDS, FSS, and EPS respectively. The corresponding areas for each scenario were 834.82 km^2, 715.46 km^2, 785.56 km^2, and 1091.43 km^2 respectively. The ecological resources in the Yinchuan Plain encompassed the Shizuishan Wetland Park, Yinchuan Wetland Park, and Wuzhong Wetland Park, all situated along the main stream of the Yellow River. Other water bod, such as Sha Lake Province Reserve, and Zhenshu Lake Wetland in northern Yinchuan Plain also contributed to ecological sources. Additionally, the forestland, including Suyukou Forest Park, Gunzhongkou Forest Park within the Helan Mountain

Nature Reserve, the wind sheltering and sand fixing forest belt on the edge of the MuUs Sandy Land and the core areas of Baijitan Nature Reserve were identified as ecological sources. The ecological sources in the Weining Plain included the core of the Shapotou Forest Farm, and Zhongwei Wetland Park in the main stream of the Yellow River. The Qingtong Canyon Bird Island Nature Reserve was located on the junction between the two plains.

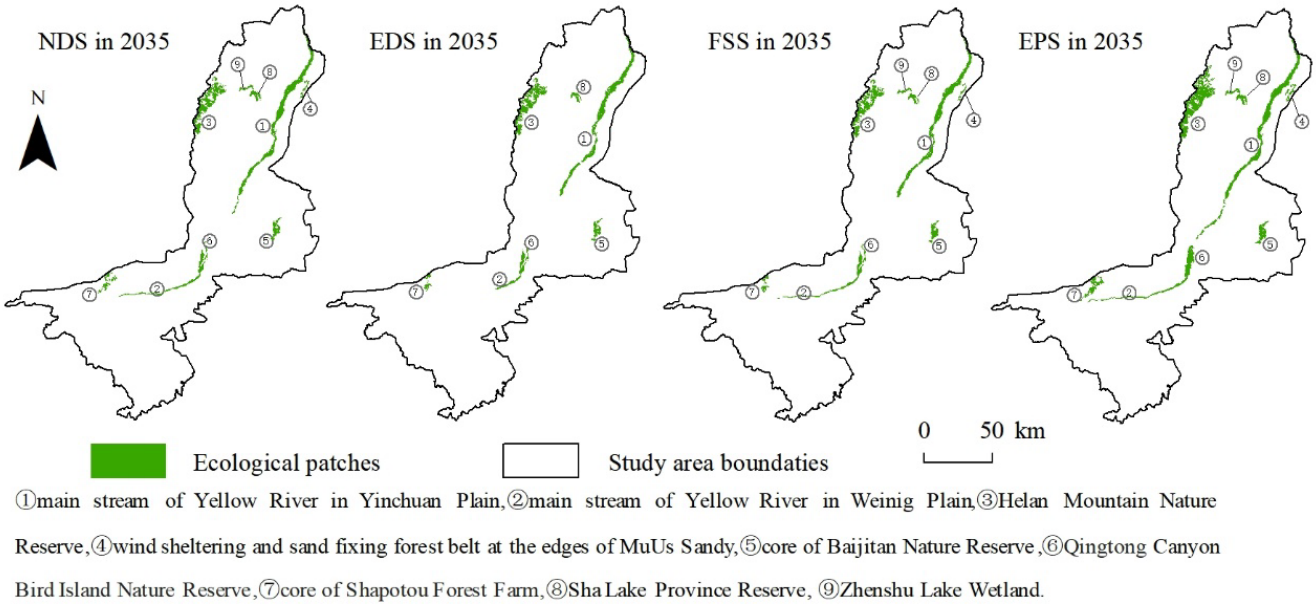


Figure 5. Ecological sources under multiple scenarios.

Compared to the other scenarios, ecological sources under the EDS exhibited the lowest numbers and areas. Additionally, certain ecological patches that fell below specified thresholds in terms of size or landscape connectivity were not classified as ecological sources. Under the EPS, the ecological sources were prominently identified. Wetlands along the main stream of the Yellow River were recognized as whole ecological sources in the Yinchuan Plain and Weining Plain, and all nature reserves were acknowledged as complete ecological sources. Under the NDS and FSS, efforts were made to identify ecological sources as completely as possible; however, there was fragmentation in terms of patch characteristics, with all ecological sources identified under the EPS being divided into several patches under NDS and FSS.

3.2.2. Ecological Resistance

According to the calculated proportions of the ecological resistance zones (Figure 6), the resistance levels decreased from the periphery zones to the center zones. Zones with the lowest and highest levels of resistance were nearly absent, while zones with medium resistance level had the greatest proportion, accounting for 61.86% of the total area, and were consistent with grassland, water body, and construction land among the land use types. The resistance would be dispersed among many ecological patches. Zones with low levels of resistance accounted for 29.57% of the total area. The resistance was located in low-elevation areas and consistent with cropland. Zones with high resistance level accounted for 8.54% of the total area. The resistance was primarily found in high-elevation areas and regions with little vegetation, including the Tengger Desert, MuUs Sandy Land, core of Baijitan, and Ningdong Energy Chemical Industry Base.

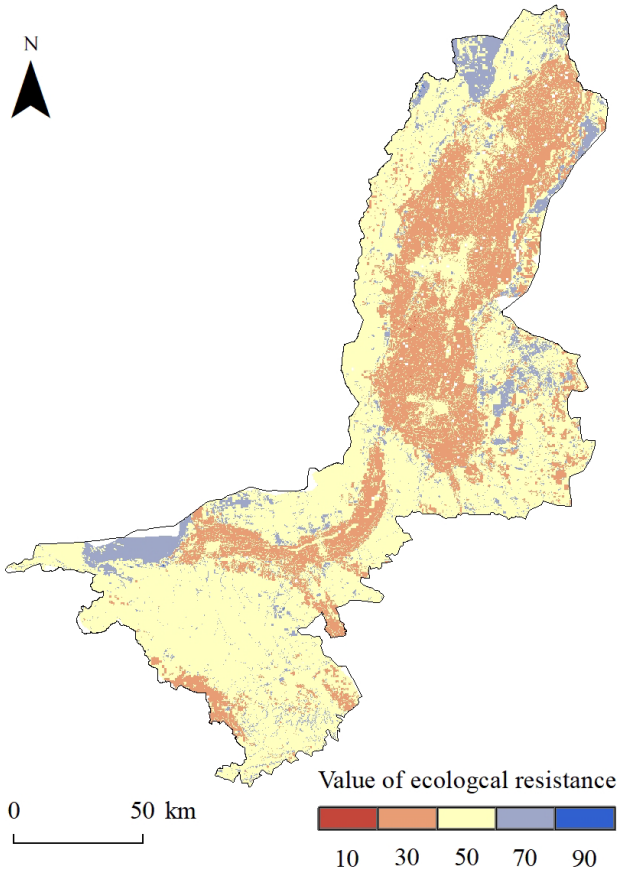


Figure 6. Surfaces indicating ecological resistance.

3.2.3. Ecological Corridors

The MCR and gravity models identified a total of 22, 14, 22, and 14 important ecological corridors with lengths of 950.01 km, 721.09 km, 1007.74 km, and 619.20 km for the NDS, EDS, FSS, and EPS respectively. In addition, there were also a total of 8, 5, 7, and 5 general ecological corridors extracted with lengths of 210.65 km, 111.61 km, 246.67 km, and 272.95 km respectively (Figure 7). The ESPs exhibited similar characteristics across the four scenarios, forming an integrated network in the Yinchuan Plain and being dispersed throughout the Weining Plain. The ecological corridors under the EPS were distributed evenly and efficiently. There were important ecological corridors connecting the Qingtong Canyon Bird Island Nature Reserve to the Helan Mountain Nature Reserve and the main stream of the Yellow River in the Yinchuan Plain. Furthermore, these ecological corridors were able to connect ecological sources in the Weining Plain. On the contrary, there was only a general ecological corridor connecting the Qingtong Canyon Bird Island Nature Reserve to the Yinchuan Wetland Park, and no ecological corridor to connect the ecological sources in the Weining Plain under the EDS. The ecological corridors under the NDS and FSS exhibited greater numbers and lengths compared to those under the EPS and EDS scenarios. This was particularly evident in the northern Yinchuan Plain, where ecological sources were dispersed throughout the region and resistance levels were relatively low.

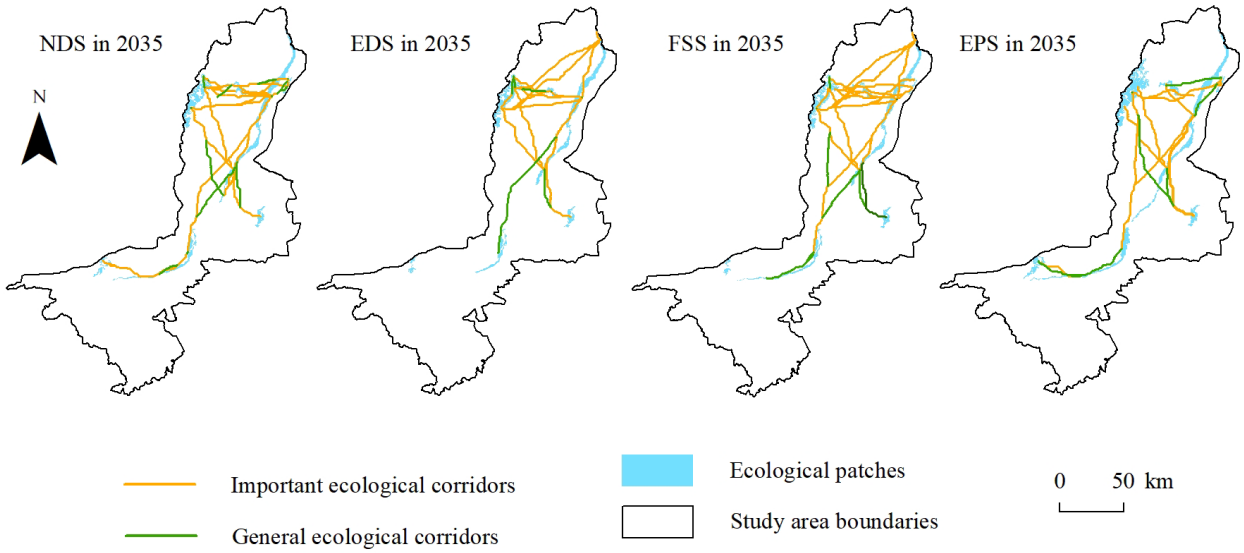


Figure 7. Ecological corridors in 2035 under multiple scenarios.

3.3. Evaluation of Network Stability of ESPs

Table 7 showed the network stability of the ESPs of the urban agglomeration along the YRB in Ningxia under multiple scenarios. Based on the ecological networks obtained from the multiple scenarios, we attempted to upgrade the general corridors into important corridors for ecological security and then calculated the metrics, depicted in Table 5. The results showed that single metrics exhibited deviations in the assessment of network stability, due to variations in evaluation factors and varying values of single metrics across different scenarios. The NDS had the highest average shortest path (I) and the lowest global efficiency (E_G) values, indicating that the higher the number of corridors, the stronger the connectivity, and the weaker the centrality. Conversely, the EDS demonstrated the opposite pattern to the NDS, with the lowest path (I) and global efficiency (E_G) values. The EPS obtained the highest overall connectivity (O_G) value; however, it exhibited lower values in single metrics compared to other scenarios, demonstrating that the comprehensive method could avoid this deficiency through the trade-offs between metrics. In addition, the numbers and lengths of ecological corridors in EPS were less than those in NDS and FSS, also indicating the importance of considering both ecological network stability and construction costs in reality.

Table 7. Network evaluation under multiple scenarios.

	NDS	EDS	FSS	EPS
k	2.000	1.900	2.071	1.580
I	11.054	18.616	13.785	14.153
E_G	3.663	13.800	4.579	8.417
cc	4.000	4.444	3.487	8.293
O_G	0.351	0.466	0.334	0.520

4. Discussion

4.1. Necessity of Simulating Future ESPs under Multiple Scenarios

The role of land use in ESPs has attracted increasing attention, indicating that the distribution of key elements of ESPs affects dynamic alterations in ecosystem structure and function. The ESP construction methods are generally divided into current and future perspectives, with the former relying on a base year and the latter relying on a future year. Compared with studies from the current perspective, the construction of ESPs from the future perspective not only maintains landscape connectivity and provides ecological value services, but also responds to future environmental change [44]. To address the

challenge of future development, it is necessary to predict various scenarios of land use with different objectives. Previous studies on ESPs in typical regions of China, such as the Pearl River Delta, Yellow River Basin, and Qinghai–Tibet Plateau, had shown that ESPs under different scenarios presented distinct spatial characteristics. Generally, the stability of ESPs decreased in the following order: EPS > NDS (BS, baseline scenario) > FSS (CLP, cultivated land protection scenario) > EDS (US, urban development scenario). However, there were significant variations in the identification results of ESPs among study areas due to environmental diversity. For example, the spatial distributions of ecological sources and corridors under the EPS were even spread throughout the Pearl River Delta, whereas in other scenarios, these components were only located in the periphery of the central region [45]. A comparison of ESPs under various scenarios revealed that the EPS predicted the best spatial structure of ecological patches and corridors for promoting material circulation and biological migration in the YRB [46]. However, effective environmental management and protection measures were still necessary to ensure a high quality and the sustainability of the entire basin [47]. The dual protection scenarios combining EPS and FSS were the best way forward in the Qinghai–Tibet Plateau [48], as ecosystem function and structure played important roles as ecological security barriers in water conservation, climate stability, and carbon balance in China, and even in Asia [49,50]. In our study, a model of "One Belt, Five Districts and Multiple Points" was developed based on the spatial distribution of ecological sources, which was similar to previous research on the same study area from a current perspective [19,51,52]. Meanwhile, it showed that coupling land use change with the construction of ESPs under multiple scenarios could balance ecological protection, urban expansion, and economic development in different areas. In the urban agglomeration along the YRB in Ningxia, the main stream of the Yellow River served as the ecological security guarantee in the area and was the focus for landscape integration and wetland biodiversity. It facilitated species migration and energy exchange in the Yinchuan Plain. Helan Mountain was designated as an ecological woodland protection zone, contributing to improved water and soil conservation through increased vegetation cover. Shapotou, MuUs Sandy Land, and Baijitan were located at the edge of deserts, leading to enhanced psammon biodiversity. Unfortunately, we identified 884.62 km^2 of ecological sources in 2018 [53], which was larger than the area of ecological sources under the NDS, EDS, and FSS but smaller than that under the EPS in 2035 in this study. Thus, it was imperative to take measure to prevent environmental deterioration due to the changes in natural and artificial factors.

In addition, based on the predictions of future land use change under multiple scenarios, we simulated carbon storage [54], habitat quality [55], urban heat island intensity [56], ecological risk [57], ecosystem services [58], and climate change [59]. In this way, if we complete the quantitative simulations of future scenarios, it could facilitate planning strategies and achieve sustainable development [60].

4.2. Proposed Development Scenario for the Future of Urban Agglomeration along the YRB in Ningxia

Based on Pepper's world hypotheses, scholars have developed a research framework for urban and regional studies, incorporating the root metaphors of correspondence, causal adjustment, organic whole, and spontaneous (history) [61]. This framework has facilitated the establishment of connections among concepts, models, and reality in our study.

Correspondence refers to the research paradigm and structure pattern of ESPs. Causal adjustment means accounting for the characteristics of the types, quantity, and spatial distribution of future land use, as well as other elements influenced by it. Organic whole refers to the formation and development of the YRB, and the role of urban agglomeration along the YRB in Ningxia. Spontaneous (history) involves implementing relevant planning schemes, policies, measures, and building engineering projects for urban agglomeration along the YRB in Ningxia. The recent paradigm of ESP construction has evolved to identify ecological sources, establish resistance surfaces, and extract corridors in theory, based on

the suitability of land use. This study integrated future land use into ESP construction. It not only reflected the continuous effects of natural and anthropogenic factors on landscapes, but also provided potential ecological pathways for improving self-regulation and ecosystem resilience. In 2021, the China Central Government issued a document—*Outline of the Yellow River Basin's Ecological Protection and High-quality Development Plan*. It emphasized steadily implementing a strategy for formulating a green way of production and living. The development design must be limited by the carrying capacity of the YRB. It should be calculated according to the simulation of land use change [62], a calculation of the environmental resource carrying capacity [63], an assessment of landscape ecological risk [64], an evaluation of vegetation restoration [65], an identification of ecological networks [46], and the optimization of urban growth boundaries [66]. The urban agglomeration along the YRB in Ningxia was located in the overlap region of Upper YRB and the Jiziwan Metropolitan Area of the YRB, which were characterized by ecological fragility and natural resource enrichment. Hence, it was essential to address the conflicts arising from ecological preservation and human activities [47], upholding the principle of the utilization of integrated water and mineral resources, agriculture and industry development within permissible limits, as well as the protection of mountains, rivers, forests, farmlands, lakes, and grasslands to prevent ecological degradation and promote ecological restoration [67]. Furthermore, it was crucial to trade off various ESPs to promote practical sustainable development [19,51].

4.3. Limitations and Future Research

The proposed framework in this study could be applied as a decision-making tool for ecological conservation by integrating land use for identifying ecological sources and extracting ecological corridors. It also has the potential to inform adjustments to development policies and management measures. However, it was notable that the study had certain limitations.

First, *dIIC* and *dPC* were utilized for a landscape connectivity analysis when identifying ecological patches. However, there is currently no standardized system for assigning values in this context [7]. In our study, we established a distance threshold of 1000 m and a connectivity probability of 0.2 based on the existing literature. Nevertheless, it was crucial to further scrutinize the reasonableness of these values.

Second, the MCR and gravity models only describe ecological corridors as line segments; in actuality, the corridors were band-like units with specific widths that vary depending on the species [68].

Third, there was a lack of a comprehensive system for assessing ecological sources. We employed landscape metrics such as percentage of landscape (PLAND), largest patch index (LPI), landscape shape index (LSI), aggregation index (AI), and landscape shape index (LSI) for evaluation. These metrics were limited to calculating the landscape structure of ecological sources from the functional perspective. However, comprehensive comparisons of the results obtained under different scenarios were not feasible.

Furthermore, the national spatial planning in China delineates three distinct types of land use—agricultural zones, ecological preservation zones, and urban development zones—through the implementation of three lines: a red line for protecting permanent basic cropland, a red line for ecological conservation, and a boundary line for urban development. It was necessary to further explore methods that can regulate the balance of these three delineated zones from a land use perspective [69].

5. Conclusions

The FLUS model, landscape ecological theory, and graph-theoretic method were employed in this study to construct ESPs under four (2035) scenarios—NDS, EDS, FSS and EPS—of urban agglomeration along the YRB in Ningxia. Subsequently, the ecological network stability were evaluated comprehensively. The primary conclusions were as follows:

The predominant land use types remained grassland and cropland, given that the study area was located in an arid or semiarid region. The forestland and water body, designated as ecological protective zones, decreased in NDS, EDS, and FSS but increased in EPS. This indicated that it was imperative to intensify ecological restoration and optimization efforts to address the threat of land use change. The spatial characteristics of the ecological sources and ecological corridors varied greatly among the different scenarios. Notably, the EPS exhibited the greatest extent of ecological sources (1091.43 km^2) and the highest overall connectivity (0.520), while it did not achieve the optimal value of single metrics and the longest ecological corridors. The results also indicated that both the ecological network stability and the construction cost should be considered. A model of "One Belt, Five Districts and Multiple Points" was developed based on the spatial distribution of ecological sources in the study. The Yellow River was the ecological security guarantee in the area, which served as the most important passageway for species migration and energy exchange. Helan Mountain was designated as an ecological woodland protection zone, while Shapotou, MuUs Sandy Land, and Baijitan were utilized to enhanced psammonphyte biodiversity.

Compared to the current perspective, this study predicted the development diversity of land use change from a future perspective. It not only responded to the various ESPs under multiple scenarios, but also balanced the contractions among the three zones delineated by the three lines for spatial planning in the future.

Author Contributions: W.C.: Conceptualization, Formal analysis, Writing—original draft. C.M.: Methodology, Supervision, Writing—review and Funding acquisition. T.L.: Methodology, Writing—review and editing. Y.L.: Software, Resources. All authors have read and agreed to the published version of the manuscript.

Funding: This research was funded by [National Natural Science Foundation of China (42061037)]. This research was also funded by [the Ningxia Science Research Project Foundation of China (2021BEG03019)]. This research was also funded by [National Science Research Project Foundation of China (2023YFF1304705)].

Data Availability Statement: Data will be made available on request.

Acknowledgments: We thank the reviewers for providing constructive comment on this manuscript. We also thank the editors for their carefully work.

Conflicts of Interest: The authors declare that they have no known competing financial interest or personal relationships that could have appeared to influence the work reported in this paper.

References

1. He, Y.; Liang, Y.; Liu, L.; Yin, Z.; Huang, J. Loss of green landscapes due to urban expansion in China. *Resour. Conserv. Recycl.* **2023**, *199*, 107228. [CrossRef]
2. Rahaman, Z.A.; Kafy, A.A.; Saha, M.; Rahim, A.A.; Almulhim, A.I.; Rahaman, S.N.; Fattah, A.; Rahman, M.T.; S, K.; Faisal, A.-A.; et al. Assessing the impacts of vegetation cover loss on surface temperature, urban heat island and carbon emission in Penang city, Malaysia. *Build. Environ.* **2022**, *222*, 109335. [CrossRef]
3. Rachman, F.; Huang, J.; Xue, X.; Marfai, M.A. Insights from 30 Years of Land Use/Land Cover Transitions in Jakarta, Indonesia, via Intensity Analysis. *Land* **2024**, *13*, 545. [CrossRef]
4. Dong, J.; Jiang, H.; Gu, T.; Liu, Y.; Peng, J. Sustainable landscape pattern: A landscape approach to serving spatial planning. *Landsc. Ecol.* **2021**, *37*, 31–42. [CrossRef]
5. Fan, X.; Cheng, Y.; Tan, F.; Zhao, T. Construction and Optimization of the Ecological Security Pattern in Liyang, China. *Land* **2022**, *11*, 1641. [CrossRef]
6. Li, X.; Chen, Y. Projecting the future impacts of China's cropland balance policy on ecosystem services under the shared socioeconomic pathways. *J. Clean. Prod.* **2020**, *250*, 119489. [CrossRef]
7. Qian, W.; Zhao, Y.; Li, X. Construction of ecological security pattern in coastal urban areas: A case study in Qingdao, China. *Ecol. Indic.* **2023**, *154*, 110754. [CrossRef]
8. Cunha, N.S.; Magalhães, M.R. Methodology for mapping the national ecological network to mainland Portugal: A planning tool towards a green infrastructure. *Ecol. Indic.* **2019**, *104*, 802–818. [CrossRef]
9. Shen, Z.; Wu, W.; Tian, S.; Wang, J. A multi-scale analysis framework of different methods used in establishing ecological networks. *Landsc. Urban Plan.* **2022**, *228*, 104579. [CrossRef]

10. Deng, Z.; Quan, B.; Zhang, H.; Xie, H.; Zhou, Z. Scenario Simulation of Land Use and Cover under Safeguarding Ecological Security: A Case Study of Chang-Zhu-Tan Metropolitan Area, China. *Forests* **2023**, *14*, 2131. [CrossRef]
11. Liu, X.; Wei, M.; Li, Z.; Zeng, J. Multi-scenario simulation of urban growth boundaries with an ESP-FLUS model: A case study of the Min Delta region, China. *Ecol. Indic.* **2022**, *135*, 108538. [CrossRef]
12. Dai, L.; Liu, Y.; Luo, X. Integrating the MCR and DOI models to construct an ecological security network for the urban agglomeration around Poyang Lake, China. *Sci Total Environ.* **2021**, *754*, 141868. [CrossRef]
13. Liang, X.; Liu, X.; Li, X.; Chen, Y.; Tian, H.; Yao, Y. Delineating multi-scenario urban growth boundaries with a CA-based FLUS model and morphological method. *Landsc. Urban Plan.* **2018**, *177*, 47–63. [CrossRef]
14. Liu, J.; Zhang, L.; Zhang, Q.; Zhang, G.; Teng, J. Predicting the surface urban heat island intensity of future urban green space development using a multi-scenario simulation. *Sustain. Cities Soc.* **2021**, *66*, 102698. [CrossRef]
15. Mao, H.; Zhou, L.; Ying, R.; Pan, D. Time Preferences and green agricultural technology adoption: Field evidence from rice farmers in China. *Land Use Policy* **2021**, *109*, 105627. [CrossRef]
16. Fang, C.; Liu, H.; Wang, S. The coupling curve between urbanization and the eco-environment: China's urban agglomeration as a case study. *Ecol. Indic.* **2021**, *130*, 108107. [CrossRef]
17. Albers, L.T.; Schyns, J.F.; Booij, M.J.; Zhuo, L. Blue water footprint caps per sub-catchment to mitigate water scarcity in a large river basin: The case of the Yellow River in China. *J. Hydrol.* **2021**, *603*, 126992. [CrossRef]
18. Jia, G.; Hu, W.; Zhang, B.; Li, G.; Shen, S.; Gao, Z.; Li, Y. Assessing impacts of the Ecological Retreat project on water conservation in the Yellow River Basin. *Sci Total Environ.* **2022**, *828*, 154483. [CrossRef]
19. Guan, H.; Bai, Y.; Tang, y.; Zhang, C.; Zou, J. Spatial identification and optimization of ecological network in desert-oasis area of Yellow River Basin, China. *Ecol. Indic.* **2023**, *147*, 109999. [CrossRef]
20. Singh, D.K.; Xu, M.; Singh, N.; Lei, F. Perspectives on emerging pressures and their integrated impact on large river systems: An insight from the Yellow River basin. *J Environ. Manag.* **2021**, *298*, 113423. [CrossRef]
21. Lyu, R.; Zhao, W.; Tian, X.; Zhang, J. Non-linearity impacts of landscape pattern on ecosystem services and their trade-offs: A case study in the City Belt along the Yellow River in Ningxia, China. *Ecol. Indic.* **2022**, *136*, 108608. [CrossRef]
22. Li, L.; Huang, X.; Wu, D.; Yang, H. Construction of ecological security pattern adapting to future land use change in Pearl River Delta, China. *Appl. Geogr.* **2023**, *154*, 102946. [CrossRef]
23. Liang, X.; Liu, X.; Li, D.; Zhao, H.; Chen, G. Urban growth simulation by incorporating planning policies into a CA-based future land-use simulation model. *Int. J. Geogr. Inf. Sci.* **2018**, *32*, 2294–2316. [CrossRef]
24. Lin, W.; Sun, Y.; Nijhuis, S.; Wang, Z. Scenario-based flood risk assessment for urbanizing deltas using future land-use simulation (FLUS): Guangzhou Metropolitan Area as a case study. *Sci Total Environ.* **2020**, *739*, 139899. [CrossRef]
25. Mondal, M.S.; Sharma, N.; Garg, P.K.; Kappas, M. Statistical independence test and validation of CA Markov land use land cover (LULC) prediction results. *Egypt. J. Remote Sens. Space Sci.* **2016**, *19*, 259–272. [CrossRef]
26. Lin, J.; He, P.; Yang, L.; He, X.; Lu, S.; Liu, D. Predicting future urban waterlogging-prone areas by coupling the maximum entropy and FLUS model. *Sustain. Cities Soc.* **2022**, *80*, 103812. [CrossRef]
27. Jokar Arsanjani, J.; Helbich, M.; Kainz, W.; Darvishi Boloorani, A. Integration of logistic regression, Markov chain and cellular automata models to simulate urban expansion. *Int. J. Appl. Earth Obs. Geoinf.* **2013**, *21*, 265–275. [CrossRef]
28. Liang, X.; Guan, Q.; Clarke, K.C.; Liu, S.; Wang, B.; Yao, Y. Understanding the drivers of sustainable land expansion using a patch-generating land use simulation (PLUS) model: A case study in Wuhan, China. *Comput. Environ. Urban Syst.* **2021**, *85*, 101569. [CrossRef]
29. Vogt, P.; Riitters, K. GuidosToolbox: Universal digital image object analysis. *Eur. J. Remote Sens.* **2017**, *50*, 352–361. [CrossRef]
30. Rincón, V.; Velázquez, J.; Gutiérrez, J.; Hernando, A.; Khoroshev, A.; Gómez, I.; Herráez, F.; Sánchez, B.; Pablo Luque, J.; García-abril, A.; et al. Proposal of new Natura 2000 network boundaries in Spain based on the value of importance for biodiversity and connectivity analysis for its improvement. *Ecol. Indic.* **2021**, *129*, 108024. [CrossRef]
31. Saura, S.; Torné, J. Conefor Sensinode 2.2: A software package for quantifying the importance of habitat patches for landscape connectivity. *Environ. Model. Softw.* **2009**, *24*, 135–139. [CrossRef]
32. Qian, W.; Li, X. A cold island connectivity and network perspective to mitigate the urban heat island effect. *Sustain. Cities Soc.* **2023**, *94*, 104525. [CrossRef]
33. Wang, T.; Li, H.; Huang, Y. The complex ecological network's resilience of the Wuhan metropolitan area. *Ecol. Indic.* **2021**, *130*, 108101. [CrossRef]
34. Huang, X.; Ye, Y.; Zhao, X.; Guo, X.; Ding, H. Identification and stability analysis of critical ecological land: Case study of a hilly county in southern China. *Ecol. Indic.* **2022**, *141*, 109091. [CrossRef]
35. Tang, Y.; Gao, C.; Wu, X. Urban Ecological Corridor Network Construction: An Integration of the Least Cost Path Model and the InVEST Model. *ISPRS Int. J. Geo-Inf.* **2020**, *9*, 33. [CrossRef]
36. Santos, J.S.; Leite, C.C.C.; Viana, J.C.C.; dos Santos, A.R.; Fernandes, M.M.; de Souza Abreu, V.; do Nascimento, T.P.; dos Santos, L.S.; de Moura Fernandes, M.R.; da Silva, G.F.; et al. Delimitation of ecological corridors in the Brazilian Atlantic Forest. *Ecol. Indic.* **2018**, *88*, 414–424. [CrossRef]
37. Nie, W.; Shi, Y.; Siaw, M.J.; Yang, F.; Wu, R.; Wu, X.; Zheng, X.; Bao, Z. Constructing and optimizing ecological network at county and town Scale: The case of Anji County, China. *Ecol. Indic.* **2021**, *132*, 108294. [CrossRef]

38. Rayfield, B.; Fortin, M.J.; Fall, A. Connectivity for conservation: A framework to classify network measures. *Ecology* **2011**, *92*, 847–858. [CrossRef]
39. Liccari, F.; Boscutti, F.; Bacaro, G.; Sigura, M. Connectivity, landscape structure, and plant diversity across agricultural landscapes: Novel insight into effective ecological network planning. *J Environ. Manag.* **2022**, *317*, 115358. [CrossRef]
40. Upadhyay, S.; Roy, A.; Ramprakash, M.; Idiculla, J.; Kumar, A.S.; Bhattacharya, S. A network theoretic study of ecological connectivity in Western Himalayas. *Ecol. Model.* **2017**, *359*, 246–257. [CrossRef]
41. Luo, Y.; Wu, J.; Wang, X.; Wang, Z.; Zhao, Y. Can policy maintain habitat connectivity under landscape fragmentation? A case study of Shenzhen, China. *Sci Total Environ.* **2020**, *715*, 136829. [CrossRef]
42. Kim, B.; Park, J. Random ecological networks that depend on ephemeral wetland complexes. *Ecol. Eng.* **2020**, *156*, 105972. [CrossRef]
43. De Montis, A.; Caschili, S.; Mulas, M.; Modica, G.; Ganciu, A.; Bardi, A.; Ledda, A.; Dessena, L.; Laudari, L.; Fichera, C.R. Urban–rural ecological networks for landscape planning. *Land Use Policy* **2016**, *50*, 312–327. [CrossRef]
44. Zhang, M.; Ao, Y.; Liu, M.; Zhao, Y.; Lin, K.; Cheng, T. Ecological security assessment based on ecosystem service value and ecological footprint in the Pearl River Delta urban agglomeration, China. *Ecol. Indic.* **2022**, *144*, 109528. [CrossRef]
45. Jiang, H.; Peng, J.; Dong, J.; Zhang, Z.; Xu, Z.; Meersmans, J. Linking ecological background and demand to identify ecological security patterns across the Guangdong-Hong Kong-Macao Greater Bay Area in China. *Landsc. Ecol.* **2021**, *36*, 2135–2150. [CrossRef]
46. Men, D.; Pan, J. Ecological network identification and connectivity robustness evaluation in the Yellow River Basin under a multi-scenario simulation. *Ecol. Model.* **2023**, *482*, 110384. [CrossRef]
47. Wei, L.; Zhou, L.; Sun, D.; Yuan, B.; Hu, F. Evaluating the impact of urban expansion on the habitat quality and constructing ecological security patterns: A case study of Jiziwan in the Yellow River Basin, China. *Ecol. Indic.* **2022**, *145*, 109544. [CrossRef]
48. Ma, R.; Zhou, W.; Ren, J.; Huang, Y.; Wang, H. Multi-scenario simulation and optimization control of ecological security based on GeoSOS-FLUS model in ecological fragile area in northeast Qinghai-Tibet Plateau, China. *Ecol. Indic.* **2023**, *151*, 110324. [CrossRef]
49. Yao, T. Tackling on environmental changes in Tibetan Plateau with focus on water, ecosystem and adaptation. *Sci. Bull.* **2019**, *64*, 417. [CrossRef]
50. Yu, Q.; Lu, H.; Yao, T.; Xue, Y.; Feng, W. Enhancing sustainability of vegetation ecosystems through ecological engineering: A case study in the Qinghai-Tibet Plateau. *J. Environ. Manag.* **2023**, *325*, 116576. [CrossRef]
51. Tang, H.; Peng, J.; Jiang, H.; Lin, Y.; Dong, J.; Liu, M.; Meersmans, J. Spatial analysis enables priority selection in conservation practices for landscapes that need ecological security. *J Environ. Manag.* **2023**, *345*, 118888. [CrossRef] [PubMed]
52. Jiang, H.; Peng, J.; Xu, D.; Tang, H. Constructing ecological security patterns with differentiated management intensity based on multifunctional landscape identification and multi-criteria decision-making. *Glob. Ecol. Conserv.* **2024**, *50*, e02862. [CrossRef]
53. Cheng, W.; Li, T.; Ma, C. Construction of an ecological security pattern based on MCR model and DO index:a case study of the ecological and economic belt along the Yellow River in Ningxia. *J. Northwest Univ. China* **2022**, *52*, 433–443.
54. Carpio, A.; Ponce-Lopez, R.; Lozano-García, D.F. Urban form, land use, and cover change and their impact on carbon emissions in the Monterrey Metropolitan area, Mexico. *Urban Clim.* **2021**, *39*, 100947. [CrossRef]
55. Yu, B.; Zang, Y.; Wu, C.; Zhao, Z. Spatiotemporal dynamics of wetlands and their future multi-scenario simulation in the Yellow River Delta, China. *J Environ. Manag.* **2024**, *353*, 120193. [CrossRef] [PubMed]
56. Lin, J.; Qiu, S.; Tan, X.; Zhuang, Y. Measuring the relationship between morphological spatial pattern of green space and urban heat island using machine learning methods. *Build. Environ.* **2023**, *228*, 109910. [CrossRef]
57. Gao, L.; Tao, F.; Liu, R.; Wang, Z.; Leng, H.; Zhou, T. Multi-scenario simulation and ecological risk analysis of land use based on the PLUS model: A case study of Nanjing. *Sustain. Cities Soc.* **2022**, *85*, 104055. [CrossRef]
58. Sun, Q.; Qi, W.; Yu, X. Impacts of land use change on ecosystem services in the intensive agricultural area of North China based on Multi-scenario analysis. *Alex. Eng. J.* **2021**, *60*, 1703–1716. [CrossRef]
59. Hanberry, B.B.; Abrams, M.D.; Nowacki, G.J. Potential Interactions between Climate Change and Land Use for Forest Issues in the Eastern United States. *Land* **2024**, *13*, 398. [CrossRef]
60. Pan, W.; Liu, Y.; Wu, Z.; Liu, Z.; Han, W.; Yu, Z. Simulation of changes in land use distribution and biodiversity under different development scenarios in Qinghai Province. *Biodivers. Sci.* **2022**, *30*, 21425. [CrossRef]
61. Yang, X. (Ed.) *Urban Remote Sensing Monitoring, Synthesis and Modeling in the Urban Environment*; Wiley & Sons, Ltd.: Hoboken, NJ, USA, 2011.
62. Lou, Y.; Yang, D.; Zhang, P.; Zhang, Y.; Song, M.; Huang, Y.; Jing, W. Multi-Scenario Simulation of Land Use Changes with Ecosystem Service Value in the Yellow River Basin. *Land* **2022**, *11*, 992. [CrossRef]
63. Chen, G.; Wang, S. Evaluation of Urban Resource Environmental Carrying Capacity and Land Spatial Development Suitability in a Semiarid Area of the Yellow River Basin. *Sustainability* **2023**, *15*, 12411. [CrossRef]
64. Du, L.; Dong, C.; Kang, X.; Qian, X.; Gu, L. Spatiotemporal evolution of land cover changes and landscape ecological risk assessment in the Yellow River Basin, 2015–2020. *J Environ. Manag.* **2023**, *332*, 117149. [CrossRef]
65. Wang, G.; Yue, D.; Niu, T.; Yu, Q. Regulated Ecosystem Services Trade-Offs: Synergy Research and Driver Identification in the Vegetation Restoration Area of the Middle Stream of the Yellow River. *Remote Sens.* **2022**, *14*, 718. [CrossRef]
66. Chen, Y.; Zhu, M.; Lu, J.; Zhou, Q.; Ma, W. Evaluation of ecological city and analysis of obstacle factors under the background of high-quality development: Taking cities in the Yellow River Basin as examples. *Ecol. Indic.* **2020**, *118*, 106771. [CrossRef]

67. Shen, W.; Li, Y.; Qin, Y. Research on the influencing factors and multi-scale regulatory pathway of ecosystem health: A case study in the Middle Reaches of the Yellow River, China. *J. Clean. Prod.* **2023**, *406*, 137038. [CrossRef]
68. Huang, L.; Wang, J.; Cheng, H. Spatiotemporal changes in ecological network resilience in the Shandong Peninsula urban agglomeration. *J. Clean. Prod.* **2022**, *339*, 130681. [CrossRef]
69. Mu, H.; Li, X.; Ma, H.; Du, X.; Huang, J.; Su, W.; Yu, Z.; Xu, C.; Liu, H.; Yin, D.; et al. Evaluation of the policy-driven ecological network in the Three-North Shelterbelt region of China. *Landsc. Urban Plan.* **2022**, *218*, 104305. [CrossRef]

Disclaimer/Publisher's Note: The statements, opinions and data contained in all publications are solely those of the individual author(s) and contributor(s) and not of MDPI and/or the editor(s). MDPI and/or the editor(s) disclaim responsibility for any injury to people or property resulting from any ideas, methods, instructions or products referred to in the content.